Environ Geochem Health (2020) 42:95–108
https://doi.org/10.1007/s10653-019-00295-6

ORIGINAL PAPER

Common and rare iron, sulfur, and zinc minerals in technogenically contaminated hydromorphic soil from Southern Russia

Yuri N. Vodyanitskii · Tatiana M. Minkina · Stanislav P. Kubrin · Denis A. Pankratov · Alexey G. Fedorenko

Received: 11 February 2019 / Accepted: 10 April 2019 / Published online: 22 April 2019

Abstract Soils formed after the desiccation of Lake Atamanskoe, which has served as a reservoir for liquid industrial waste from the city of Kamensk-Shakhtinsky during a long time, were studied. These soils differ from zonal soils by a strong contamination with zinc and sulfur. Preliminary studies showed that Fe compounds fix a significant part of zinc. This requires to study S, Zn, and Fe minerals. In this work, Mössbauer spectroscopy was used for the identification of iron compounds and scanning electron microscopy was used for the microanalysis of these and other minerals. To facilitate the identification of Fe minerals, brown iron ocher was removed from a contaminated soil sample and analyzed. From electron microscopy and Mössbauer spectroscopy data, ocher contained hydrogoethite with a high content of sorption water and schwertmannite (a rare mineral, probably found in Russia for the first time). The chemical composition of this schwertmannite better corresponds to the Cashion–Murad model than to the Bigham model. Particles of partially oxidized magnetite and wustite enriched with zinc were revealed under electron microscope. Siderite with partial substitution of Fe^{2+} by Zn^{2+} was detected. Thus, contaminated hydromorphic soil contains both common minerals (illite, goethite, hematite, gypsum) and rare minerals (schwertmannite, Zn siderite, partially oxidized magnetite and wustite enriched with zinc).

Keywords Illite · Goethite · Hematite · Gypsum · Schwertmannite · Zn siderite · Partially oxidized magnetite · Zn wustite · Scanning electron microscopy · Mössbauer spectroscopy

Y. N. Vodyanitskii · D. A. Pankratov
Lomonosov Moscow State University, Moscow, Russia 119991
e-mail: yu.vodyan@mail.ru

D. A. Pankratov
e-mail: pankratov@radio.chem.msu.ru

T. M. Minkina (✉) · S. P. Kubrin
Southern Federal University, Rostov-on-Don, Russia 344006
e-mail: tminkina@mail.ru

S. P. Kubrin
e-mail: stasskp@gmail.com

A. G. Fedorenko
Southern Federal University, Southern Scientific Center of Russian Academy of Sciences, Rostov-on-Don, Russia 344006
e-mail: afedorenko@mail.ru

Introduction

Technogenically contaminated soils differ from zonal soils by the frequent presence of unusual minerals. These minerals have different origins. Some of them get into the soil together with solid-phase pollutants. An example is provided by badlands contaminated with sulfides from ore dumps in the southern Urals

(Vodyanitskii et al. 2018). Other unusual minerals form in the soil during the hydrogenic contamination with liquid pollutants, e.g., in the soils formed during the desiccation of Lake Atamanskoe, which has served as a reservoir for industrial waste from the city of Kamensk-Shakhtinsky, Rostov oblast, for a long time (from the 1950s to the early 1990s).

The soil formed during the desiccation of Lake Atamanskoe is strongly enriched with zinc and sulfur (Minkina et al. 2018). The contents of zinc and sulfur exceed their lithosphere clarks in up to 800 and 80 times, respectively. Of interest is the composition of Zn- and S-containing compounds in this technogenic soil. Among authigenic minerals of the Atamanskoe Lake, the share of sulfates is high (45–60%), although the mineralogy of sulfates is not ascertained (Minkina et al. 2018). From sequential chemical extraction data, Zn mainly occurs in silicates (45–49%); the second major fraction is Zn fixed by Fe minerals (22–31%); the following fractions are Zn bound to organic compounds (6–13%) and Zn in carbonates (5–7%) (Minkina et al. 2018). The early used optical methods gave no clear answer on the composition of newly formed S and Zn minerals in this soil. The composition of Fe minerals as Zn and S carriers should also be considered because of the significant share of Zn fixed by minerals. In this context, we attempted to extend the range of analytical methods for revealing Fe, S, and Zn minerals. Scanning electron microscopy was used, as well as Mössbauer spectroscopy oriented only to the analysis of Fe minerals. The color of iron ocher in the CIELab system was also determined as an additional parameter of Fe minerals.

Beginning from the 1970s, scanning electron microscopy serves as the main tool in soil micromorphology. It is used for studying elementary soil-forming processes: weathering of primary minerals, illuviation of finely dispersed material, gleization, and development of Al–Fe humus process (Shoba 2007). However, the study is generally reduced to the visual analysis of the surface of particles and aggregates. Electron microscopes are equipped with an X-ray analyzer capable of determining many chemical elements in the particle under study. However, the chemical analysis of particles is not always used. For example, only the presence of Fe and O was noted in the study of Fe particles, but the mineral composition of particles was not examined (Pronina 2007; Zagurskii 2008). However, magnetite and maghemite shells or schwertmannite, goethite, and ferrihydrite globules cannot be distinguished by their shape alone, although these minerals differ in chemical composition.

We attempted to use chemical analysis data to identify the mineralogy of particles containing Fe, S, and Zn by electron microscopy and to agree the results of other analyses of technogenically contaminated hydromorphic soil. However, a number of methodological problems should be solved for the determination of the chemical composition of minerals. The aim of this work was to study common and rare Fe, S, and Zn compounds in a technogenically contaminated hydromorphic soil.

Objects

Lake Atamanskoe is located in the Severskii Donets floodplain. This is an oxbow of Severskii Donets, the main tributary of the Don River (48°20′42.15″N, 40°14′14.46″E). Lake Atamanskoe was used as a reservoir for industrial wastes released from the chemical plant from the early 1960s to the 1990s. The lake contains 180,000 tons of flowing silts, 343,000 tons of low-plastic silts, and 444,000 tons of high-plastic silts (Privalenko et al. 2000). All these sediments are contaminated with heavy metals and organometallic compounds. In terms of contents of many heavy metals, primarily Zn, these technogenic oozes could be ascribed to rich ores, and their volumes are large enough for the large-scale exploration of technogenic ores (Privalenko et al. 2000). A change in hydrological conditions for the past 20–30 years due to the termination of industrial runoffs and longer-term dry period led to the lake evaporation and, correspondingly, caused an active soil formation. The study objects are the technogenically transformed soils (Spolic Technosols) located in the territory of former Atamanskoe Lake: plots D1–D4.

Soil samples

Sampling was performed according to ISO 10381-1 (2002). In each monitoring plot, samples were collected from the upper 0–20 cm layer. Samples were stored in polyethylene bags and transported to the laboratory. Soil samples were air-dried in a special

room without chemical reagents at a temperature of 20–24 °C and a relative humidity of 60–70%.

The main physical and chemical characteristics of the soil were determined by an accredited analysis laboratory (Certificate No. ROSS RU 0001.511127) following International Standard Organization methods (ISO Guide 34 2009). Properties of the studied soil samples and the content of Zn and SO_3 in them are given in Table 1.

Isolation of ocher

To facilitate the identification of Fe minerals, brown iron ocher (the color of the air-dry sample) was removed from the contaminated soil sample D3 and analyzed using Mössbauer spectroscopy and scanning electron microscopy. Samples of contaminated soil for analysis were separated by direct magnet. Magnetic field strength is 2.137 kOe. For this purpose, soil samples were mixed with water at a ratio of 1:10. A ferrite magnet was put into the obtained mixture and collected iron-containing particles. Then, the separator was withdrawn from the mixture, put into another container with pure water, and isolated from electricity. This series of operations was repeated several times, and an enriched mixture was thus obtained in the second container, which was dried and studied by Mössbauer spectroscopy and scanning electron microscopy.

Methods

Physical and chemical properties of the studied soil samples were analyzed by the commonly used standard method for the Russian Federation (Vorob'eva 2006): The exchangeable bases were determined with 1 M NH_4OAc, the pH was measured by potentiometry, organic matter content was determined by potassium dichromate digestion, soil texture was determined by the pipette method, cation exchange capacity was determined by the ammonium acetate method, and carbonates were determined by titrimetric analysis and dense water extract residue. The total content of Zn and SO_3 in the soils was determined by X-ray fluorescent scanning spectrometer "SPECTROSCAN MAKC-GV".

Mössbauer spectroscopy

Mössbauer absorption spectra were measured on MS1104EM electrodynamic-type with a spectrometer. Measurements were performed under constant acceleration mode in moving source geometry with the speed change in a triangular pattern ^{57}Co in Rh matrix used as γ-ray source. The samples were cooled in Janis CCS-850 helium cryostat refrigerator. The models fitting for experimental spectra were performed using SpectRelax software (Matsnev and Rusakov 2012). Isomer shifts are described relative to the α-Fe.

Table 1 Physical and chemical properties of Spolic Technosols of the monitoring plots

Parameter	Monitoring plots			
	D1	D2	D3	D4
C_{org}, %	2.8 ± 0.2	3.6 ± 0.2	2.4 ± 0.1	4.4 ± 0.2
pH_{water}	7.7 ± 0.1	7.8 ± 0.2	8.0 ± 0.2	7.7 ± 0.3
$CaCO_3$, %	7.8 ± 0.2	5.7 ± 0.2	3.8 ± 0.2	5.3 ± 0.3
Exchangeable Ca^{2+}, cmol(+)/kg	29.2 ± 2.0	30.0 ± 2.2	27.3 ± 1.9	35.2 ± 1.7
Exchangeable Mg^{2+}, cmol(+)/kg	4.8 ± 0.1	5.1 ± 0.1	4.3 ± 0.1	5.0 ± 0.2
Clay (< 1.0 μm), %	18.8 ± 1.6	17.9 ± 1.5	25.4 ± 1.9	33.0 ± 2.6
Zn content, mg/kg	25973.7 ± 1780.5	3672.5 ± 304.0	66075.4 ± 7095.0	62032.1 ± 5903.0
SO_3 content, %	4.3 ± 0.03	5.6 ± 0.02	7.1 ± 0.1	7.3 ± 0.1

Scanning electron microscopy

Mineral composition has been determined from the total contents of chemical elements since long ago. The identification of minerals with a constant chemical composition like quartz, hematite, and ilmenite poses no problems. The chemical composition determined under electron microscope also allows identifying simple minerals. However, this causes problems of two kinds. First, this is the identification of particles containing minerals with different oxidation states of chemical elements (Mn and Fe minerals). In this work, it was interesting to identify particles containing Fe minerals with different degrees of Fe oxidation. Second, there are problems with minerals containing sorption water. Even in minerals with a fixed composition containing sorption water, e.g., gypsum $CaSO_4.2H_2O$, distortions of chemical composition can be due to the partial loss of sorption water under microscope's vacuum and electron irradiation.

Minerals containing sorption water, including silicates, are widely distributed in soils. One of them is allophane; the uncertainty of its chemical composition is described by the formula $xSiO_2{\cdot}yAl_2O_3{\cdot}zH_2O$. Another mineral of uncertain composition is montmorillonite (Ca, Mg,…) (Al, Fe^{3+}, $Mg)_2(OH)_2[(Si, Al)_4O_{10}]nH_2O$ (Sokolova et al. 2005). Thus, the identification of silicates faces problems because of the uncertain content of water.

Particle shape determined under microscope is insufficient for the identification of minerals. For example, spherical shape is typical not only for ferrihydrite particles, but also for goethite nanoparticles (Angelico et al. 2014). Such an additional parameter as chemical composition of particles should be used.

Iron oxides

In some of these minerals, Fe has different degrees of oxidation, which complicates their identification from chemical composition. Spherical magnetic particles of complex structure occur in soils. Their degree of oxidation increases from the center to the surface in the following order: Fe → FeO → Fe_3O_4 → Fe_2O_3 → FeOOH (Ivanov 2003). Real particles contain a narrower range of these minerals, usually two or three minerals. For identification, the rule of stages should also be considered: Only adjacent minerals of the above series can coexist in spherical Fe particles. The rule of oxidation stages was followed for the composition of spherical particles in the studied soils. Particles composed of wustite (FeO) partially oxidized to magnetite (Fe_3O_4) were revealed, as well as particles of magnetite (Fe_3O_4) partially oxidized to maghemite (γFe_2O_3).

Hydrogoethite

The composition of nanogoethite particles differs from the composition of stoichiometric goethite (FeOOH), because they contain sorption water, which is described by the conventional formula $FeOOH.nH_2O$. To identify nanogoethite from the composition chemical of microparticles, the content of oxygen, which depends on the degree of hydration, should be known.

The natural diversity of goethites involves the different degrees of Fe substitution and the different degrees of hydration, which affect the size and shape of crystals. Goethites containing more water than monohydrate are referred to as hydrogoethites. In hydrogoethites studied by Bagin et al. (1988), the content of water reached $n = 1.6H_2O$. Slightly hydrated particles (up to 0.5 H_2O) have an acicular shape with a maximum crystal size up to 150 nm; strongly hydrated particles (up to 40–70 nm in size) have a collomorphic structure. However, this is not the limit degree of goethite dispersion; an even finer mineral (2–12 nm), which is called nanogoethite, occurs in sediments on the bottoms of Canadian lakes (Van der Zee et al. 2003). The degree of hydration of hydroxides increases with increasing degree of dispersion; therefore, the extrapolation of Bagin's data on the content of free water for particles of 150 nm to particles of ∼ 10 nm gives the approximate formula $FeOOH{\cdot}2H_2O$ for nanogoethites.

Schwertmannite

The structure and chemical composition of schwertmannite remain open to question. It is presently believed that the structure of schwertmannite is analogous to that of akaganeite with the tunnel configuration of octahedrons FeO_6 (Barham 1997; Fernandez-Martinez et al. 2010; Cui et al. 2011; Lu et al. 2013). In an experiment with the addition of sulfate to synthetic akaganeite, eight diffraction lines'

characteristics of schwertmannite were obtained (Bigham et al. 1990). Under electron microscope, aggregates of schwertmannite nanoparticles have a hedgehog-like shape (Parafiuk and Siuda 2006).

There is no common opinion on the chemical composition of schwertmannite. Bigham et al. (1994) were the first to propose the chemical formula $Fe_8O_8(OH)_{8-x}(SO_4)_x$, where x varies from 1 to 1.75. Later on, it was shown that x varies from 1.74 to 1.86 (Yu et al. 1999). Thus, according to Bigham, the approximate formula of schwertmannite is $Fe_8O_8(OH)_{6.2}(SO_4)_{1.8}$. Cashion and Murad (2012) proposed another approximate formula for schwertmannite: $Fe_8O_8(OH)_6SO_4$. The formulas differ in the molecular Fe/S ratio. In the specified Bigham formula, Fe/S = 7.8; in the Cashion–Murad formula, Fe/S = 14.0. Parafiuk and Siuda (2006) reported data on the chemical composition of schwertmannite formed in acid drainage water sediments of a sulfide mine in western Sudetes, Poland. Schwertmannite is a key solid in removing acidity in treatment systems where Fe^{2+} is rapidly oxidized by addition of alkalinity to acid mine drainage (Gagliano et al. 2004; Fernandez-Martinez et al. 2010).

The chemical composition of schwertmannite was determined by electron microscopy EDS X-ray microanalysis. Let us consider the compositions of two schwertmannite samples differing in the Fe/S ratio: It is 9.6 for sample 1 with the lower iron content and 12.1 for sample 2 with the higher iron content. Thus, the actual Fe/S ratio in schwertmannite is higher than that in the Bigham formula and lower than that in the Cashion–Murad formula.

The chemical formulas of real schwertmannite samples from Poland according to the Bigham and Cashion–Murad formulas are given in Table 2. For sample 2 the content of oxygen in the Bigham formula is so low that the O/Fe ratio in the octahedral lattice of schwertmannite become lower than 1. The Cashion–Murad model does not show such a serious violation of schwertmannite structure, which suggests that this model is preferable. In the structure of schwertmannite under electron microscope, the share of hydroxyl groups is lower than stoichiometric because of oxygen loss; i.e., the number of OH groups is 5 for low-iron schwertmannite and 3.5 for high-iron mineral, rather than 6 as in the Cashion–Murad model. Thus, in electron microscope, the molecule of schwertmannite loses 1–2.5 OH groups. It might be expected that OH groups can also be lost by the electron microscopy microanalysis of schwertmannite in the studied samples of technogenically contaminated hydrogenic soil.

Results and discussion

Iron minerals

Mössbauer spectroscopy

Mössbauer spectra at room temperature of intact soil samples are shown in Fig. 1. At room temperature, the spectra of all samples consist of two paramagnetic doublets A and B; sample 3 also includes sextet C. Hyperfine parameters of these spectra are given in Table 3. The parameters of sextet C corresponds to ions Fe^{3+} in hematite (Murad 2010; Vandenberghe and De Grave 2013; Wagner and Wagner 2004). The isomer shift (δ) of doublet A corresponds to ions Fe^{3+}, and that of doublet B corresponds to ions Fe^{2+} (Pankratov 2014). The parameters of doublets A and B approximately coincide with those in the Mössbauer spectrum of illite (Murad and Wagner 1994).

However, Fe occurs in soil samples in the form of nanoparticles of different oxides and hydroxides. The detected phases exhibit superparamagnetic properties at room temperature. Thus, the magnetic moments of iron ions spontaneously change their direction. Superparamagnetism results in the collapse of Zeeman lines in the Mössbauer spectrum into a doublet or a singlet

Table 2 Chemical formulas of schwertmannite in sediments of acid drainage water from a sulfide mine according to the Cashion–Murad and Bigham models

N	Elements			Models	
	O	Fe	S	Bigham	Cashion–Murad
1	0.35	0.59	0.06	$Fe_8O_8(OH)_{0.4}(SO_4)_{1.8}$	$Fe_8O_8(OH)_{5.0}SO_4$
2	0.34	0.61	0.05	$Fe_8O_{7.2}(SO_4)_{1.8}$	$Fe_8O_8(OH)_{3.5}SO_4$

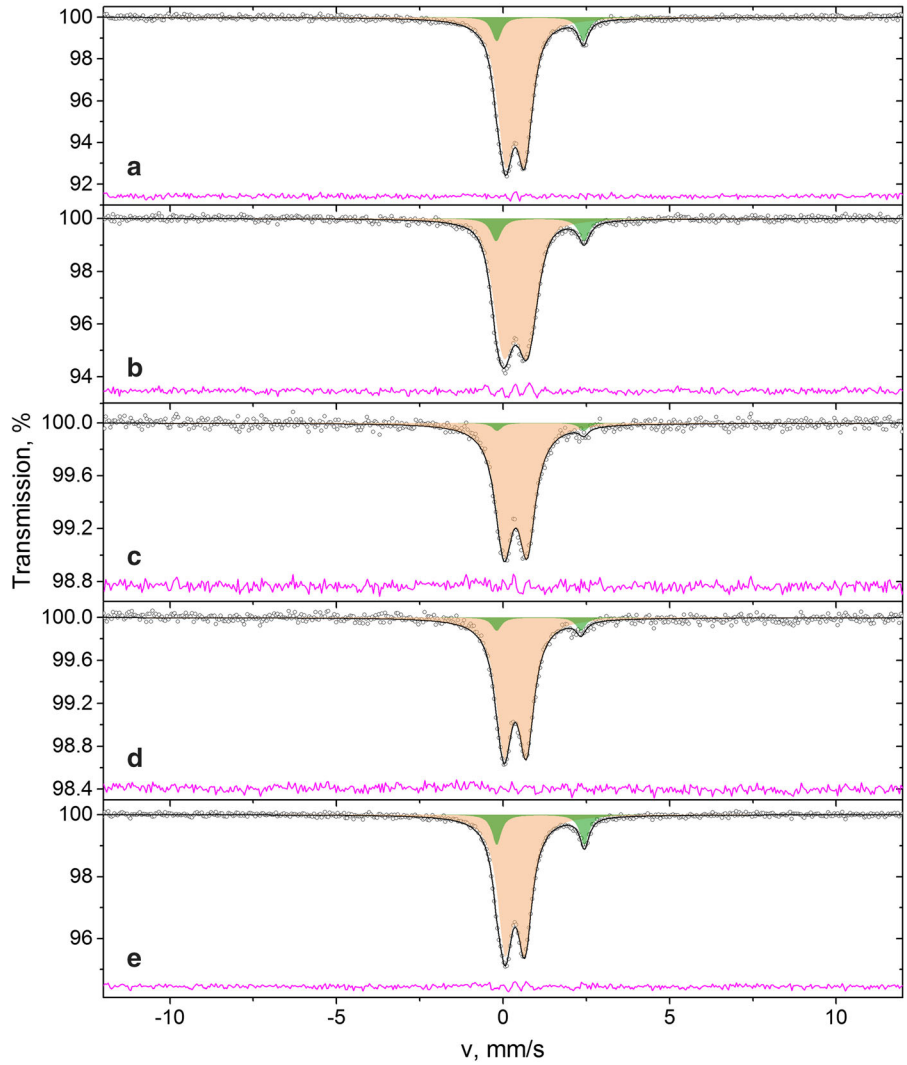

Fig. 1 Mössbauer spectra's of soil samples and ocher measured at room temperature: **a** D1; **b** D2; **c** D3; **d** D4; **e** ocher

(Bedanta and Kleemann 2009). Thus, doublet A can also correspond to Fe^{3+} ions from highly dispersed iron oxides or hydroxides (Murad 2010; Vandenberghe and De Grave 2013; Wagner and Wagner 2004). To distinguish Fe^{3+} ions in illite from highly dispersed iron oxides and hydroxides, the effect of superparamagnetism on the structure of Mössbauer spectra should be eliminated. Measurements at low temperatures were performed for this purpose.

Mössbauer spectra of samples measured at a temperature of 14 K are shown in Fig. 2, Tables 3 and 4. In addition to doublets A and B, Zeeman sextets C and D appear in the spectra at low temperature. The parameters of sextet C approximately coincide with those of the Mössbauer spectrum of hematite nanoparticles (Murad 2010; Vandenberghe and De Grave 2013; Wagner and Wagner 2004). The δ value of sextet D corresponds to Fe^{3+} ions in the octahedral oxygen surrounding (Pankratov 2014). The hyperfine magnetic field is lower than that of sextet C corresponding to hematite. Sextet D may be equivalent to goethite (α-FeOOH) (Murad 2010; Vandenberghe and De Grave 2013; Wagner and Wagner 2004).

For Mössbauer spectra of ocher sample, it should be noted that when the temperature falls, the doublet A area significantly decreases and the doublet B area remains unchanged within the error. Thus, doublet A at room temperature corresponds to Fe^{3+} ions in illite

Table 3 Parameters of Mössbauer spectra of Spolic Technosols of the monitoring plots

Sample	T (K)	Component	$\delta \pm 0.01$ (mm/s)	$\varepsilon/\Delta \pm 0.02$ (mm/s)	H ± 1 (kOe)	G ± 0.02 (mm/s)	S± (%)	Fe state	χ^2
D1	300	A	0.36	0.58		0.58	90	Fe^{3+} in illite and goethite	1.003
		B	1.11	2.60		0.35	10	Fe^{2+} in illite	
	14	A	0.47	0.54		0.62	70	Fe^{3+} in illite	1.087
		B	1.26	2.82		0.32	8	Fe^{2} in illite	
		C	0.48	− 0.09	461	0.48	22	Fe^{3+} in goethite	
D2	300	A	0.37	0.62		0.72	90	Fe^{3+} in illite and goethite	1.299
		B	1.11	2.6		0.39	10	Fe^{2+} in illite	
	14	A	0.48	0.54		0.7	60	Fe^{3+} in illite	1.214
		B	1.29	2.80		0.52	8	Fe^{2+} in illite	
		C	0.48	− 0.09	477	0.8	32	Fe^{3+} in goethite	
D3	300	A	0.38	0.68		0.62	96	Fe^{3+} in illite and goethite	1.166
		B	1.12	2.60		0.34	4	Fe^{2+} in illite	
	14	A	0.46	0.60		0.58	41	Fe^{3+} in illite	1.211
		B	1.12	2.60		0.41	13	Fe^{2+} in illite	
		C	0.48	− 0.021	462	1.34	46	Fe^{3+} in goethite	
D4	300	A	0.36	0.66		0.57	94	Fe^{3+} in illite and goethite	1.191
		B	1.07	2.52		0.34	6	Fe^{2+} in illite	
	14	A	0.45	0.64		0.65	39	Fe^{3+} in illite	1.288
		B	1.1	2.62		0.4	6	Fe^{2+} in illite	
		C	0.49	− 0.05	454	1.79	55	Fe^{3+} in goethite	

δ, Isomer shift; ε, quadrupole shift; Δ, quadrupole splitting for paramagnetic components; H, hyperfine magnetic field on 57fe nucleus; A, component area; G, line width

and superparamagnetic goethite and ferrihydrite. The fitting of the Mössbauer spectra for ocher at 14 K revealed four components, including doublet A: Fe^{3+} in illite containing 60% of total Fe; doublet B: Fe^{2+} in illite containing 11% Fe; sextet C: Fe^{3+} in goethite containing 14% Fe; and sextet E containing 15% Fe (Fig. 2, Table 4). The last component corresponds to Fe^{3+} ions; its hyperfine magnetic field is lower than for the sextets corresponding to hematite and goethite. This sextet can be due to Fe^{3+} ions in ferrihydrite or schwertmannite (Cashion and Murad 2012; Frye, ed. 1983). The obtained results do not allow exactly determining the type of Fe mineral. To elucidate the situation, let us examine an additional ocher parameter: color.

Ocher color analysis

It provides some clarity on the mineralogy of component E. The color of ocher in the Munsell system is 7.5 YR 4/4, which corresponds to lightness $L^* = 41.2$, redness $a^* = 10.0$, and yellowness $b^* = 23.6$ on the CIELab color space. Thus, the redness of ocher is relatively high: Red = $a/(a + b) = 0.30$. To compare, the mean values for other minerals are as follows: Red = 8.2/(8.2 + 44.1) = 0.16 for yellow goethite, Red = 15.4/(15.4 + 34.9) = 0.31 for ferrihydrite, and Red = 16.0/(16.0 + 48.0) = 0.25 for schwertmannite. Thus, ocher should contain red pigments. This is not phase A, B, or C. Consequently, one of two red minerals (ferrihydrite or schwertmannite) should be present in component D.

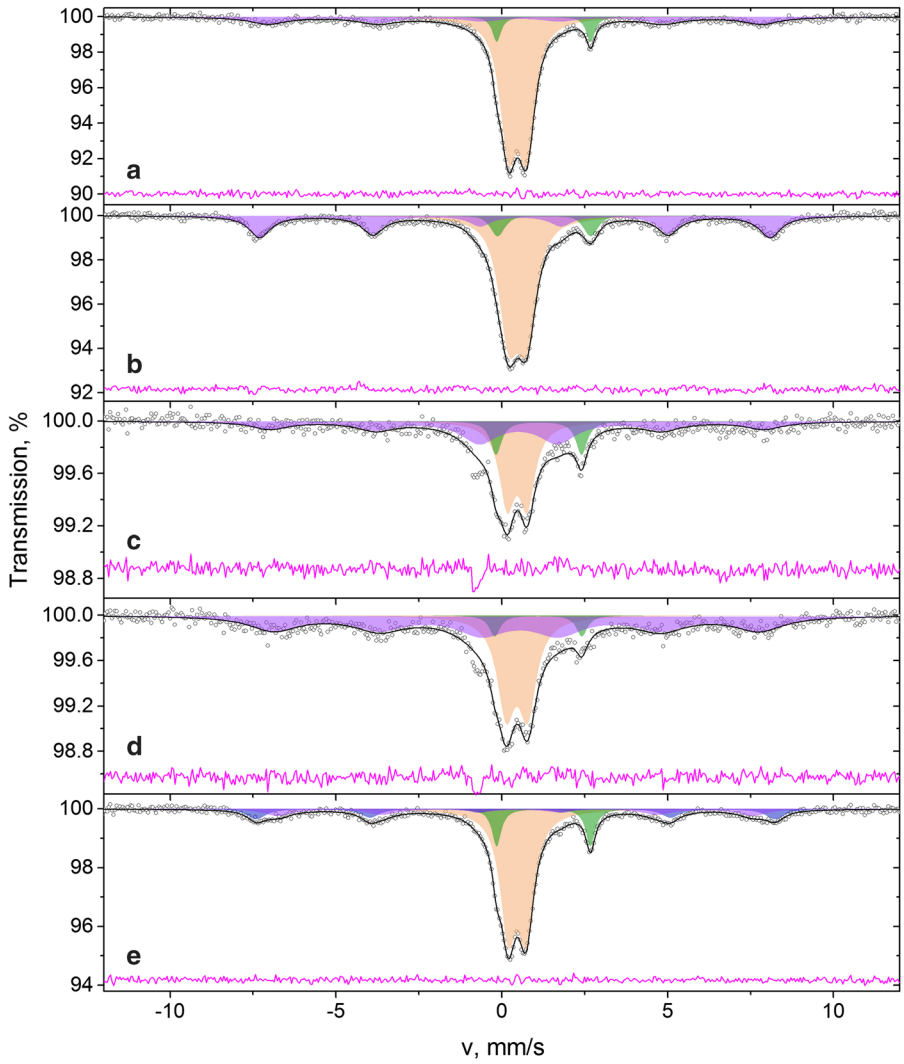

Fig. 2 Mössbauer spectra of soil samples and ocher measured at a temperature of 14 K: **a** D1; **b** D2; **c** D3; **d** D4; **e** ocher

Table 4 Mössbauer spectra of ocher sample

T (K)	Component	$\delta \pm 0.02$ (mm/s)	$\Delta/\varepsilon \pm 0.02$ (mm/s)	H ± 1 (kOe)	S ± 1 (%)	G ± 0.02 (mm/s)	χ^2	Fe state
300	A	0.36	0.59		0.54	86.5	1.194	Fe^{3+} illite/goethite
	B	1.13	2.64		0.34	13.5		Fe^{2+} illite
14	A	0.46	0.54		0.58	59.7	1.046	Fe^{3+} illite
	B	1.26	2.82		0.34	11.5		Fe^{2+} illite
	C	0.49	− 0.07	485	0.68	14		Fe^{3+} goethite
	D	0.47	− 0.07	444	1.06	14.9		Fe^{3+} schwertmannite

δ, Isomer shift; ε, quadrupole shift; Δ, quadrupole splitting for paramagnetic components; H, hyperfine magnetic field on 57fe nucleus; A, component area; G, line width

The genesis of soil should be taken into consideration in the consideration of fine disordered Fe hydroxides with similar parameters of Mössbauer spectra. It is important that the soil has formed from bottom sediments after the desiccation of Lake Atamanskoe. This hydromorphic soil could inherit Fe minerals remained under reducing conditions. It is known that ferrihydrite, the least stable Fe hydroxide with the maximum specific surface area, is first subjected to reduction under reducing conditions (Roden and Zachara 1996). Goethite, but not ferrihydrite, remained in sedimentary deposits of Canadian lakes (Van der Zee et al. 2003). This is an argument for the presence of yellow goethite, as well as red ocher pigment schwertmannite rather than ferrihydrite, in the studied hydromorphic soils.

Electron microscopy microanalysis of ocher

Iron oxides

The identification of minerals is possible only for particles of homogeneous composition and containing three–four chemical elements (Zahid et al. 2009), for example, O, Fe, and Zn (spectrum 2 and 3); O, S, and Ca (spectrum 6 and 7); O, S, and Fe (spectrum 1 and 8); O, Si, Fe, and Zn (spectrum 4); and C, O, Fe, and Zn (spectrum 5) (Fig. 3). However, the mineralogy of particles with more complex chemical composition is difficult to determine: O, Si, S, Ca, Fe, and Zn (spectrum 9) or O, Al, Si, K, and Fe (spectrum 10) (Fig. 4).

Iron oxides in ocher consist of magnetite partially oxidized to maghemite (Table 5). Some Fe oxide particles contain Zn inclusions. In sample 3, wustite is partially oxidized to Zn magnetite, and sample 2 consists of Zn goethite. In sample 4, Fe hydroxides occur as nanosized particles of hydrogoethite sorbing Zn and Si. Note that the Mössbauer spectra did not reveal magnetite, maghemite, or wustite. The reason was that the concentrations of these minerals were significantly lower than the concentrations of the main Fe phases: hematite, goethite, and illite.

Thus, Zn is present in oxides or hydroxides, including magnetite and hydrogoethite. The siderophilicity of Zn is one of its manifestations in soils, especially hydromorphic soils, where the synthesis of Fe minerals occurs in the presence of large amounts of Zn (Manceau et al. 2000, 2003; Manceau et al. 2004). The enrichment of Zn minerals in spinel, e.g., substitution of Zn^{2+} for Fe^{2+} in the magnetite lattice, is also well known (Kudryavtseva 1988). Preliminary studies showed that a significant part of Zn is fixed in Fe compounds (Minkina et al. 2018).

Carbonates

A Zn siderite ($Zn_{0.2}Fe_{0.8}CO_3$) is revealed in ocher (Table 5, Fig. 5). It forms in soils more rarely than calcite does. Zavarzina (2001) simulated the formation of siderite in soils. Under reducing conditions at the constant CO_2 concentration (20%), two Fe(II) phases form in the gas phase: magnetite and siderite. A high Fe concentration in the system is favorable for magnetite, and a low concentration is favorable for siderite. The increase in the content of CO_2 in the system favors an increase in the content of newly formed siderite. Thus, the presence of magnetite and siderite in ocher of hydrogenic soil is well expectable. Their combination is due to the strong variation of redox potential in the soil (Barham 1997). The identification of magnetite and siderite by Mössbauer spectroscopy is impossible because of their relatively low share among Fe minerals. In siderite, Fe^{2+} is partially substituted by Zn^{2+} (Table 5). This is a common process in siderites (Frye, ed. 1983).

Sulfates

Two sulfate types are revealed: widely distributed and well-studied gypsum and a rare Fe hydroxysulfate schwertmannite.

Gypsum

Gypsum is the dominant sulfate in this contaminated soil. The content of sorption water in gypsum determined under microscope depends of the size of particles. In particle 7 with a clear prismatic shape, the composition of gypsum corresponds to the stoichiometric formula $CaSO_4 \cdot 2H_2O$. In dispersed gypsum particle 6 with uncertain morphology, only one molecule of sorption water is detected under microscope (Table 5, Fig. 6).

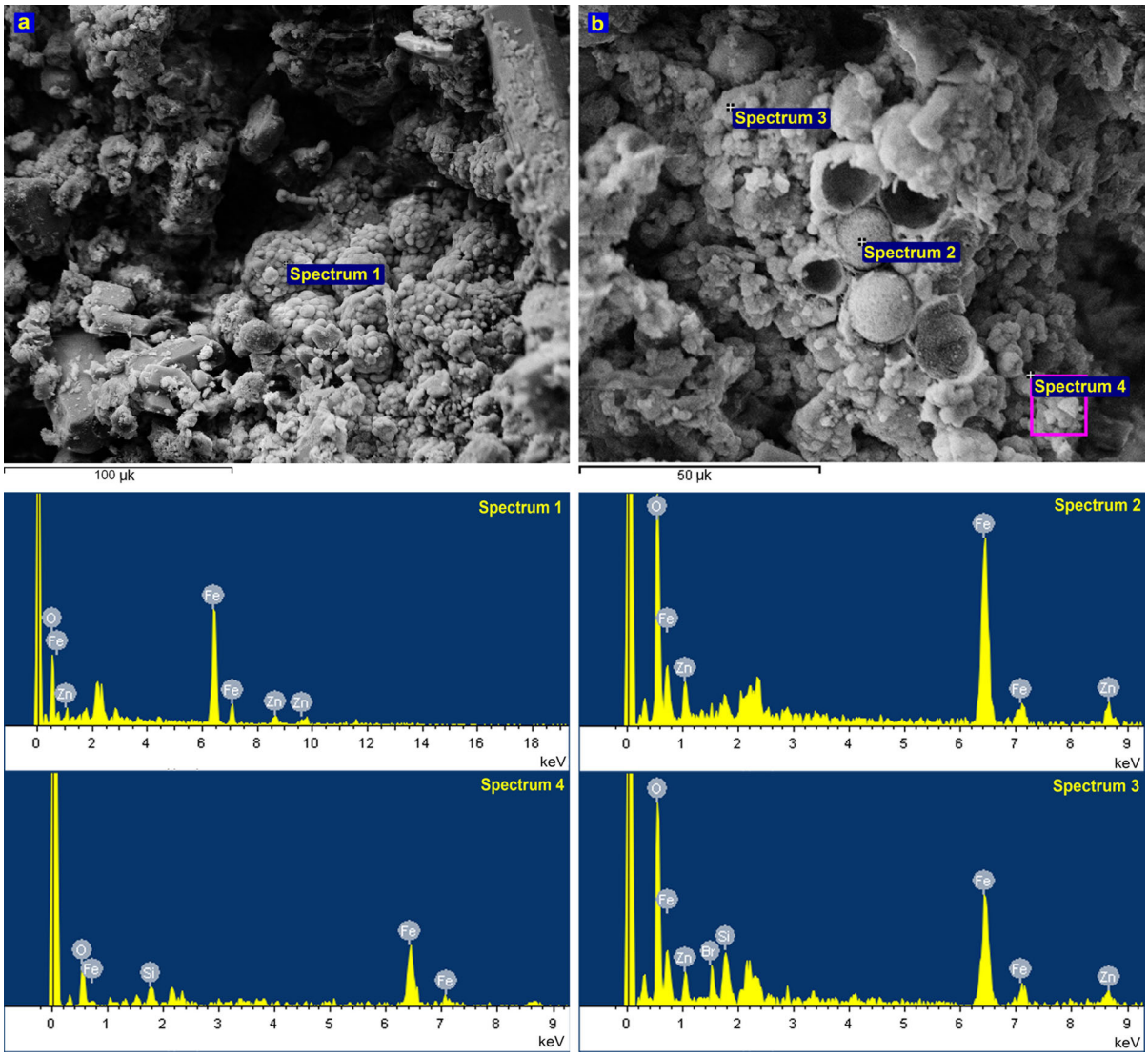

Fig. 3 Electron microscopy microanalysis of iron oxides complex chemical composition in ocher. **a** Spectrum 9, **b** spectrum 10

Schwertmannite

This poorly crystallized iron oxyhydroxysulfate is poorly known. It is precipitated as ocher on sulfide-enriched rocks and in contaminated soils. It is also deposited on the bottom of brooks and lakes contaminated with acid mine drainage waters enriched with SO_4 and Fe^{2+} (Fernandez-Martinez et al. 2010). Aggregates of schwertmannite nanoparticles thus form under the effect of atmospheric air with the participation of microorganisms in oxidative conditions (Fernandez-Martinez et al. 2010). Schwertmannite is the main mineral formed during the neutralization of acid mine drainage waters (Parafiuk and Siuda 2006). Less dates are available about the formation of schwertmannite under natural conditions: on the bottoms of acidified lakes and in waterlogged soils and bogs (Burton et al. 2007; Parafiuk and Siuda 2006). However, schwertmannite was recognized as a mineral only recently, despite of its important role in geochemical processes (Bigham et al. 1990). The reason is its difficult identification because of poor crystallization and common association with more crystalline phases like goethite and jarosite. The instability of schwertmannite also complicates its identification: The mineral can transform to goethite

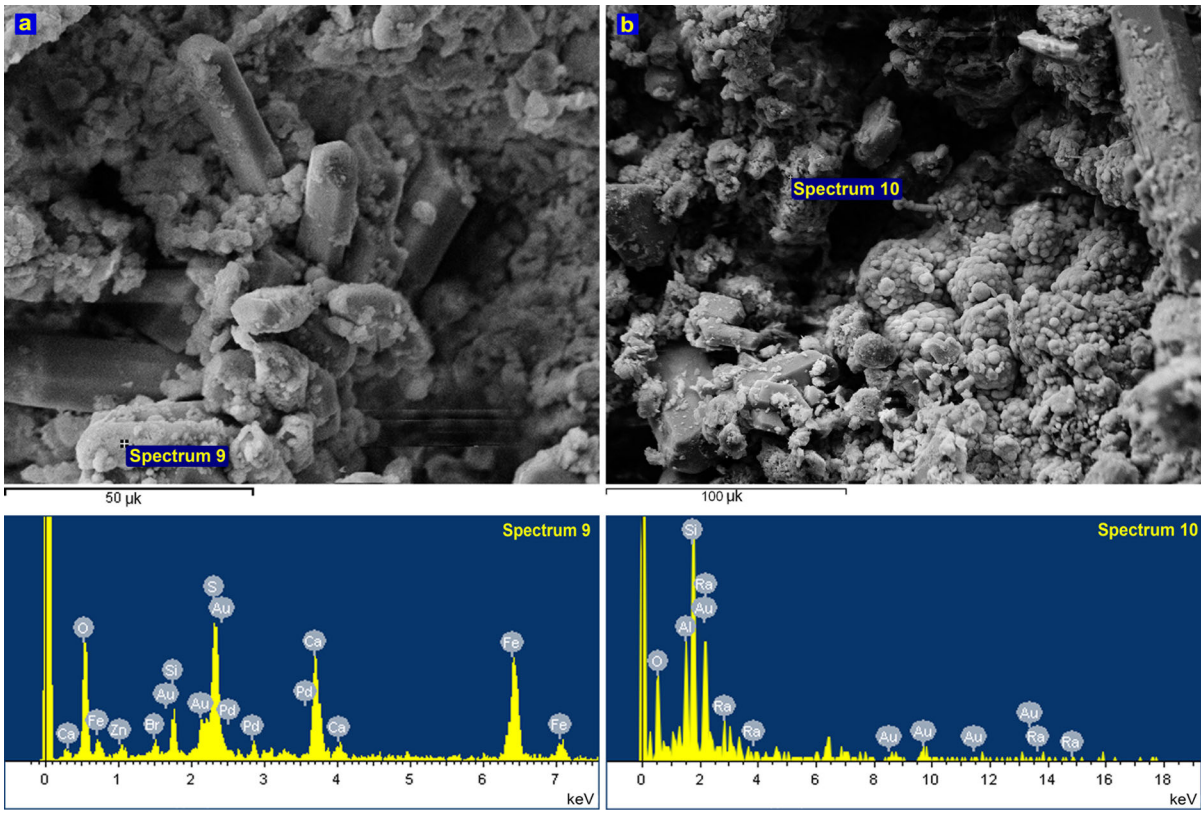

Fig. 4 Electron microscopy microanalysis of iron oxides in ocher. **a** Spectrum 3, **b** spectrum 2, spectrum 3, spectrum 4

Table 5 Mineral composition of particles of ocher according to electron microscopy

No spectrum	C	O	S	Si	Fe	Zn	Ca	Mineral	Proof
Fe oxides									
1		0.29			0.71			Magnetite partially oxidized to maghemite	
2		0.33			0.54	0.12		$Zn_{0.2}FeOOH$	
3		0.22			0.65	0.13		Zn goethite	
4		0.46		0.05	0.39	0.10		$Si_{0.2}Zn_{0.2}FeOOH{\cdot}2H_2O$	From MS, goethite with H = 485 kOe at 14 K
Carbonates									
5	0.12	0.43			0.35	0.10		$Zn_{0.2}Fe_{0.8}CO_3$	
Sulfates									
6		0.51	0.23				0.25	$CaSO_4{\cdot}H_2O$	
7		0.57	0.20				0.23	$CaSO_4{\cdot}2H_2O$	
8		0.26	0.06		0.68			$Fe_8O_8SO_4$	From MS, schwertmannite with H = 444 kOe at 14 K

and jarosite within several months (Acero et al. 2006; Bigham et al. 1996).

Sample 8 consists of schwertmannite (Table 5, Fig. 6). According to the Cation–Murad model, its formula is $Fe_8O_8SO_4$. This means that all OH groups

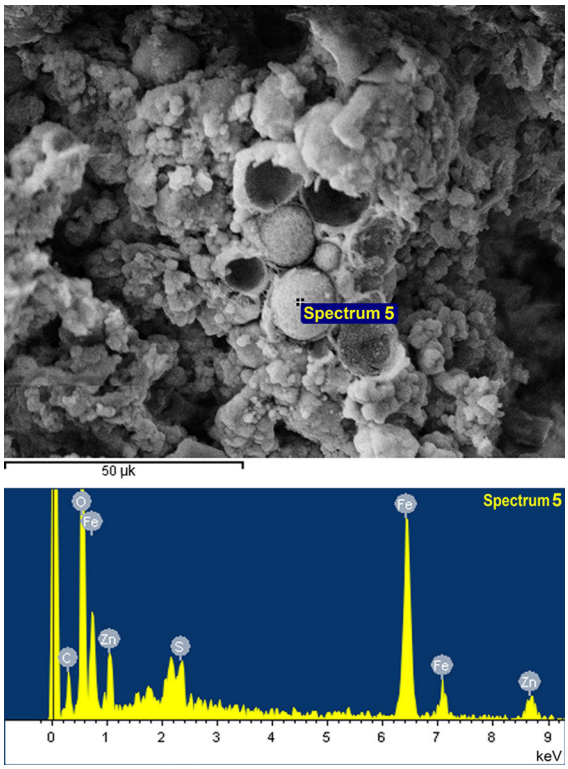

Fig. 5 Electron microscopy microanalysis of carbonates in ocher. Spectrum 5

of unstable schwertmannite are lost in electron microscope. Ferrihydrite particles are not revealed in ocher; therefore, sextet D of Mössbauer spectrum can be considered as appropriate of schwertmannite.

Conclusions

Mineralogy in contaminated soils is frequently more complex than in zonal soils due to rare, untypical minerals. This is confirmed by the formation of soils after the desiccation of Lake Atamanskoe, which has served as a reservoir of liquid industrial waste from the city of Kamensk-Shakhtinsky for a long time. These soils differ from zonal soils by a strong contamination with Zn and S.

Mössbauer spectroscopy was used for the identification of iron compounds, and scanning electron microscopy was used for the detection of these and other minerals. To improve the identification accuracy of Fe minerals, brown iron ocher was removed from the contaminated soil sample.

The electron microscopy microanalysis and ^{57}Fe Mössbauer spectroscopy data revealed the presence of hydrogoethite with a large amount of water and the rare mineral schwertmannite (probably found in Russia for the first time) in ocher. The chemical composition of schwertmannite better corresponds to the Cation–Murad model than to the Bigham model.

Electron microscopy also revealed particles of partially oxidized magnetite and wustite enriched with Zn. Siderite with the partial substitution of Zn^{2+}

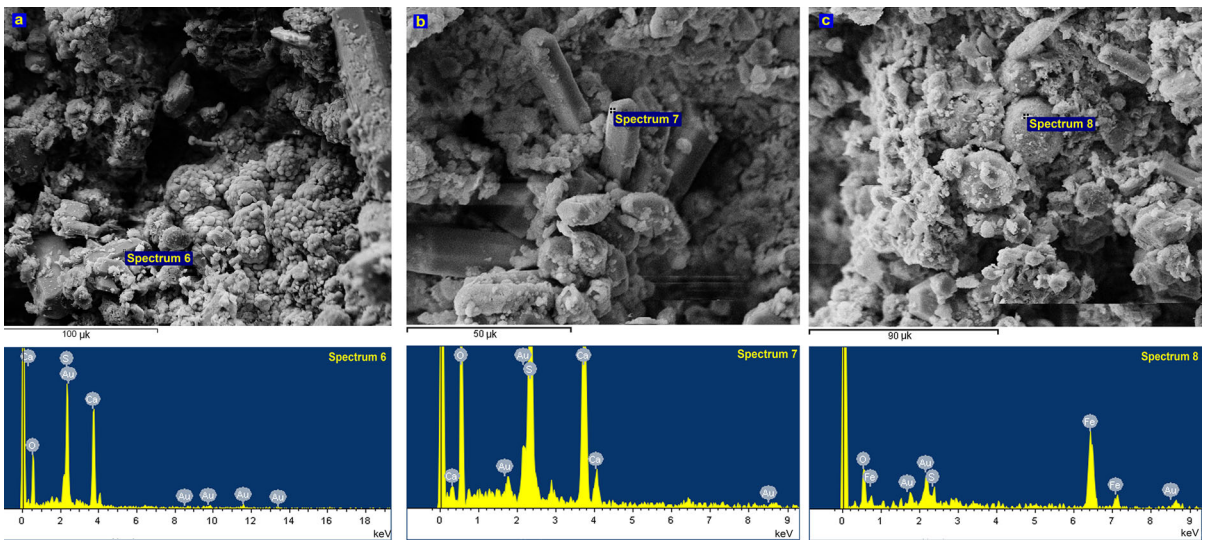

Fig. 6 Electron microscopy microanalysis of sulfates in ocher. **a** Spectrum 6, **b** spectrum 7, **c** spectrum 8

for Fe^{2+} was also detected. Sulfates in the contaminated soils occurred as gypsum particles.

Both common minerals (illite, goethite, hematite, gypsum) and rare minerals (schwertmannite, Zn siderite, partially oxidized magnetite and wustite enriched with zinc) were revealed in the contaminated hydromorphic soil.

Acknowledgements This work was supported by the Ministry of Education and Science of Russia, Project No. 5.948.2017/PCh, Russian Academy of Sciences, Project No. AAAA-A19-119011190176-7.

Compliance with ethical standards

Conflict of interest The authors declare that they have no conflict of interest.

References

Acero, P., Ayora, C., Torrento, C., & Nieto, J. M. (2006). The behavior of trace elements during schwertmannite precipitation and subsequent transformation into goethite and jarosite. *Geochimica et Cosmochimica Acta, 70,* 4130–4139.

Angelico, R., Ceglie, A., Ji-Zheng, H., Yu-Rong, L., Palumbo, G., & Colombo, C. (2014). Particle size, charge and colloidal stability of humic acids coprecipitated with ferrihydrite. *Chemosphere, 99,* 239–347.

Bagin, B. I., Gendler, T. S., & Avilova, T. A. (1988). *Magnetism of iron α-oxides and hydroxides*. Moscow: Akademiya Nauk SSSR.

Barham, R. J. (1997). Schwertmannite: A unique mineral, contains a replaceable ligand, transforms to jarosites, hematites, and/or basic iron sulfate. *Journal of Materials Research, 12,* 2751–2758.

Bedanta, S., & Kleemann, W. (2009). Supermagnetism. *Journal of Physics D: Applied Physics, 42,* 013001.

Bigham, J. M., Carlson, L., & Murad, E. (1994). Schwertmannite, a new iron oxyhydroxysulphate from Pyhasalmi, Finland, and other localities. *Mineralogical Magazine, 58,* 641–648.

Bigham, J. M., Schwertmann, U., Carlson, L., & Murad, E. (1990). A poorly crystalli-zed oxyhydroxysulfate of iron formed by bacterial oxidation of Fe(II) in acid-mine waters. *Geochimica et Cosmochimica Acta, 54,* 2743–2758.

Bigham, J. M., Schwertmann, U., Traina, S. J., Winland, R. L., & Wolf, M. (1996). Schwertmannite and the chemical modeling of iron in acid sulfate waters. *Geochimica et Cosmochimica Acta, 60,* 2111–2121.

Burton, E. D., Bush, R. T., Sullivan, L. A., & Mitchell, D. R. G. (2007). Reductive transformation of iron and sulfur in schwertmannite-rich accumulations associated with acidified coastal lowlands. *Geochimica et Cosmochimica Acta, 71,* 4456–4473.

Cashion, J. D., & Murad, E. (2012). Mössbauer spectra of the acid mine drainage mineral schwertmannite from the Sokolov basin, Czech Republic. In *Proceedings of the 36th annual condensed matter and materials meeting, Wagga, NSW, Australia*, TP30:1–TP30:4.

Cui, M., Jang, M., Cho, S.-H., & Khim, J. (2011). Potential application of sludge produced from coal mine drainage treatment for removing Zn(II) in an aqueous phase. *Environmental Geochemistry and Health, 33,* 103–112. https://doi.org/10.1007/s10653-010-9348-0.

Fernandez-Martinez, A. V., Nimon, V., Roman-Ross, G., Cuello, G. J., Daniels, J. E., & Ayora, C. (2010). The structure of schwertmannite, a nanocrystalline iron oxyhydroxysulfate. *American Mineralogist, 95,* 1312–1322.

Frye, K. (Ed.). (1983). *The encyclopedia of mineralogy*. Berlin: Springer.

Gagliano, W. B., Brill, M. R., Bigham, J. M., Jones, F. S., & Traina, S. J. (2004). Chemistry and mineralogy of ochreous sediments in a constructed mine drainage wetland. *Geochimica et Cosmochimica Acta, 68,* 2119–2128.

ISO 10381-1. (2002). *Soil quality*. Sampling. Part 1. Guidance on the Design of Sampling Programs.

ISO Guide 34. (2009). *General Requirements for the Competence of Reference Material Producers*.

Ivanov, A. V. (2003). *Magnetic and valent state of iron in soil solid phase*. Doctoral (Biology) Dissertation, Moscow: Moscow State University.

Kudryavtseva, G. P. (1988). *Ferrimagnetism of natural oxides*. Moscow: Nedra.

Lu, W., Lin, Ch., & Ma, Yi. (2013). Long-term geochemical evolution of acidic mine wastes under anaerobic conditions. *Environmental Geochemistry and Health, 35,* 523–533. https://doi.org/10.1007/s10653-013-9512-4.

Manceau, A., Lanson, B., Schlegel, M. L., Harge, J. C., Musso, M., Eybert-Berard, L., et al. (2000). Quantitative Zn speciation in smelter-contaminated soils by EXAFS spectroscopy. *American Journal of Science, 300,* 289–343.

Manceau, A., Marcus, M. A., Tamura, N., Proux, O., Geoffroy, N., & Lanson, B. (2004). Natural speciation of Zn at the micrometer scale in a clayey soil using X-ray fluorescence, absorption, and diffraction. *Geochimica et Cosmochimica Acta*, *68*(11), 2467–2483. https://doi.org/10.1016/j.gca.2003.11.021.

Manceau, A., Tamura, N., Celestre, R. S., Macdowell, A. A., Geoffroy, N., Sposito, G., et al. (2003). Molecular-scale speciation of Zn and Ni soil ferromanganese nodules from loess soils of the Mississippi Basin. *Environmental Science and Technology, 37,* 75–80.

Matsnev, M. E., & Rusakov, V. S. (2012). SpectrRelax: An application for Mössbauer spectra modeling and fitting. *American Institute of Physics Conference Proceedings, 1489,* 178–185.

Minkina, T., Nevidomskaya, D., Bauer, T., Shuvaeva, V., Soldatov, A., Mandzhieva, S., et al. (2018). Determining the speciation of Zn in soils around the sediment ponds of chemical plants by XRD and XAFS spectroscopy and sequential extraction. *Science of the Total Environment, 634,* 1165–1173.

Murad, E. (2010). Mössbauer spectroscopy of clays, soils and their mineral constituents. *Clay Minerals, 45,* 413–430.

Murad, E., & Wagner, U. (1994). The Mössbauer spectrum of illite. *Clay Minerals, 26,* 1–10.

Pankratov, D. A. (2014). Mössbauer study of oxo derivatives of iron in the Fe_2O_3-Na_2O_2 system. *Inorganic Materials, 50,* 82–89.

Parafiuk, J., & Siuda, R. (2006). Schwertmannite precipitated from acid mine drainage in the Western Sudetes (SW Poland) and its arsenate sorption capacity. *Geological Quarterly, 50*(4), 475–486.

Privalenko, V. V., Mazurenko, V. T., Panaskov, V. I., Moshkin, V. M., Mukhin, N. V., & Senin, B. K. (2000). *Ecological problems in the city of Kamensk-Shakhtinsk*. Rostov-on-Don: Tsvetnaya pechat'.

Pronina, V. V. (2007). *Formation of magnetic iron oxides in soils at the underground storage of natural gas*. Candidate (Biology) Dissertation. Moscow: Moscow State University.

Roden, E. E., & Zachara, J. M. (1996). Microbial reduction of crystalline Fe(III) oxides: Influence of oxide surface area and potential for cell growth. *Environmental Science and Technology, 30,* 1618–1628.

Shoba, S. A. (2007). *Morphogenesis of taiga-zone soils*. Moscow: NIA-Priroda.

Sokolova, T. A., Dronova, T. Ya., Tolpeshta, I. I. (2005). *Clay minerals in soils*. Tula: Grif.

Van der Zee, C., Roberts, D. R., Rancourt, D. G., & Stomp, C. P. (2003). Nanogoethite is the dominant reactive oxyhydroxide phase in lake and marine sediments. *Geology, 31,* 993–996.

Vandenberghe, R. E., & De Grave, E. (2013). Chapter 3. Application of Mössbauer spectroscopy in earth sciences. In Y. Yoshida & G. Langouche (Eds.), *Mössbauer spectroscopy* (pp. 91–185). Berlin: Springer.

Vodyanitskii, Yu. N., Minkina, T. M., Kubrn, S. P., Linnik, V. G. (2018). Iron sulphides and their effect on the XRF measurement of the bulk chemical composition of badland soils near the Karabash copper smelter, Southern Urals, Russia. *Geochemistry: Exploration, Environment, Analysis*. https://doi.org/10.1144/geochem2017-081.

Vorob'eva, L. A. (2006). *Theory and practice chemical analysis of soils*. Moscow: GEOS.

Wagner, F. E., & Wagner, U. (2004). Mössbauer spectra of clays and ceramics. *Hyperfine Interactions, 154,* 35–82.

Yu, J. Y., Heo, B., Choi, I. K., Cho, J. P., & Chang, H. W. (1999). Apparent solubilities of schwertmannite and ferrihydrite in natural stream waters polluted by mine drainage. *Geochimica et Cosmochimica Acta, 63,* 3407–3416.

Zagurskii, A. M. (2008). *Specific macrostructure and genesis of magnetic iron compound sin soils*. Candidate (Biology) Dissertation, Moscow: Moscow State University.

Zahid, A., Hassan, M. Q., Breit, G. N., Balke, K.-D., & Flegr, M. (2009). Accumulation of iron and arsenic in the Chandina alluvium of the lower delta plain, Southeastern Bangladesh. *Environmental Geochemistry and Health, 31,* 69–84. https://doi.org/10.1007/s10653-008-9226-1.

Zavarzina, N. G. (2001). *Biogeochemical factors of iron compound transformation under reducing conditions*. Candidate (Geology, Mineralogy) Dissertation, Moscow: Moscow State University.